Two-photon absorption cross sections: An investigation of solvent effects. Theoretical studies on formaldehyde and water

Martin J. Paterson,[a] Jacob Kongsted,[b] and Ove Christiansen[c]
Department of Chemistry, University of Århus, Langelandsgade 140, DK-8000 Århus C, Denmark

Kurt V. Mikkelsen[d] and Christian B. Nielsen[e]
Department of Chemistry, University of Copenhagen, Universitetsparken 5, DK-2100 Copenhagen Ø, Denmark

(Received 2 June 2006; accepted 22 September 2006; published online 8 November 2006)

The effects of a solvent on the two-photon absorption of microsolvated formaldehyde and liquid water have been studied using hybrid coupled-cluster/molecular mechanics (CC/MM) response theory. Both water and formaldehyde were considered solvated in water, where the solvent water molecules were described within the framework of molecular mechanics. Prior to the CC/MM calculations, molecular dynamics simulations were performed on the water/formaldehyde and water/water aggregates and many configurations were generated. By carrying out CC/MM response calculations on the individual configurations, it was possible to obtain statistically averaged results for both the excitation energies and two-photon absorption cross sections. For liquid water, the comparison between one- and two-photon absorption spectra is in good agreement with the experimental data available in the literature. In particular, the lowest energy transition occurring in the one-photon absorption spectrum of water only occurs with a relatively small strength in the two-photon absorption spectrum. This result is important for the interpretation of two-photon absorption data as these results show that in the absence of selection rules that determine which transitions are forbidden, the spectral profile of the two-photon absorption spectrum can be significantly different from the spectral profile of the one-photon absorption spectrum. © *2006 American Institute of Physics*. [DOI: 10.1063/1.2363997]

I. INTRODUCTION

Theoretical predictions of two-photon absorption (TPA) cross sections have recently received an increasing interest. In particular, efforts have been made to model the TPA cross section of a series of organic molecules.[1–6] The molecules studied were molecules with potential use for three-dimensional (3D) microfabrication, molecular machines, and also photodynamic cancer therapy.[7–18] However, the theoretical levels used for calculating the cross sections are typically comparatively low level. Furthermore, the calculations are invariably performed in the gas phase, not including any description of a surrounding medium, though a quantum mechanical-molecular mechanics investigation on the TPA of liquid water has appeared utilizing a molecular dynamics averaged water structure.[19] It is also important to note that determination of accurate experimental TPA cross sections is a difficult task, which is exemplified for the molecule shown in Fig. 1, where cross sections of 3670×10^{-50}, 1940×10^{-50}, 1890×10^{-50}, and 15.4×10^{-50}cm^4 s have been measured by several groups.[5,20,21] Even for a simple water molecule, experimentally determined cross sections span two orders of magnitude.[22–26] This large spread in the experimentally determined numbers sometimes makes it difficult to compare theoretical and experimental results.

In recent papers we have presented calculations of TPA cross sections of gas-phase water and formaldehyde,[27,28] where we have investigated the necessary theoretical level for obtaining accurate cross sections for a single molecule. We have also investigated solvent effects on the TPA cross sections of liquid water using the multiconfigurational self-consistent field/molecular mechanics approach.[19] With an understanding of the effects of dynamic correlation and one-particle basis set error on calculated TPA cross sections, we have in the present work investigated the effects of solvation on this nonlinear molecular property. To this end we have used the coupled-cluster/molecular mechanics (CC/MM) response method which allows inclusion of large numbers of configurations (solute-solvent geometries), necessary for ob-

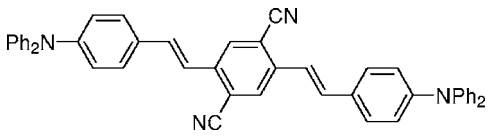

FIG. 1. A chromophore (*E*,*E*-2,5-dicyano-1,4-bis[2-(4-diphenylamino-phenyl)-vinyl]-benzene) studied by several groups in two-photon absorption experiments.

[a]Present address: School of Engineering and Physical Sciences, Heriot-Watt University, Edinburgh, EH14 4AS, Scotland. Electronic mail: m.j.paterson@hw.ac.uk
[b]Electronic mail: kongsted@chem.au.dk
[c]Electronic mail: ove@chem.au.dk
[d]Electronic mail: kmi@theory.ki.ku.dk
[e]Author to whom correspondence should be addressed; present address: Laboratory of Macromolecular and Organic Chemistry, Eindhoven University of Technology, P.O. Box 513, 5600 MB, Eindhoven (The Netherlands). Electronic mail: chr@kiku.dk

 © 2006 American Institute of Physics

Downloaded 08 Nov 2006 to 137.195.101.208. Redistribution subject to AIP license or copyright, see http://jcp.aip.org/jcp/copyright.jsp

taining a statistically converged value for the TPA cross section. A MM treatment of the solvent molecules (each solvent molecule is described with an effective charge on each atom and an isotropic polarizability assigned to the oxygen site of the solvent molecule) has in several cases been shown to correctly describe the correct short- and long-range physics of solvation, whereas in the dielectric continuum model only the long-range bulk effects are correctly modeled.[29,30]

Formaldehyde is the simplest molecule containing a carbonyl group. Of particular interest with regards to TPA are organic molecules containing carbonyl groups which have great potential as singlet oxygen photosensitizers due to their rather efficient intersystem crossing (according to El-Sayed's selection rules), producing the lowest triplet state of the sensitizing molecule (which in turn can transfer its excitation energy to ground state oxygen yielding singlet oxygen).[31,32] Designing two-photon singlet oxygen sensitizers has been the topic of some of our recent research.[4,33–36]

Water presents a molecule where solvation through hydrogen bonding affects the molecular properties significantly. In the gas phase, we have found that it is a difficult task to obtain a converged TPA cross section for a single water molecule. This is due to the diffuse nature of the excited states in water: A significant Rydberg character is present in the excited states of water which makes it crucial to use highly diffuse basis sets in accurate calculations. The expression for the TPA transition moment contains a summation over all the excited electronic states[37] in the molecule (*vide infra*), making the calculated TPA cross sections very sensitive to the diffuse nature of the basis set. In comparison to water, the $n \rightarrow \pi^*$ excited state of formaldehyde does not contain any significant Rydberg character and properties such as the TPA cross sections are thus more easily converged in terms of the theoretical level used, although (at least) a single set of diffuse functions is still necessary.[27]

The present work is concerned with solvation effects on the TPA cross section of water and formaldehyde. Both molecules are considered solvated in water, which is a polar solvent and forms a strong cooperative hydrogen bonding network. Due to these two properties, it is a significant challenge to model solvation effects for molecules solvated in water. The model used to calculate the TPA cross section for the solvated molecule is the CC/MM model with CC2 (coupled-cluster wave function including single excitations and an approximate treatment of double excitations[38]) or CCSD (coupled-cluster wave function including single and double excitations[39]). Prior to the CC/MM calculations, a molecular dynamics simulation was carried out, and configurations were dumped every picosecond for 1.2 or 1.5 ns long simulations. A CC/MM response calculation was then carried out for every configuration. An average of the excitation energies, TPA and one-photon absorption cross sections for all the configurations included were then calculated. In the present work, we discuss the TPA cross sections in terms of convergence as a function of the number of configurations included in the calculations. For formaldehyde, we investigate the effect of treating solvent molecules quantum mechanically. Thus, we present results of calculations where statistical averaging is performed for an ensemble of a solute, described with quantum mechanics, and a significant number of water molecules (approximately 140–160) described with molecular mechanics. We also investigated the effect of including one and two solvent molecules in the "quantum mechanical aggregate" on the calculated cross section. Comparisons with experimentally determined cross sections are also made, although, as alluded to above, the direct comparison with absolute values is problematic, so we will focus on changes in the theoretical spectral profiles (i.e., spectral shifts and quenching or enhancement of particular absorption bands) induced by solvation. In addition, for liquid water, comparison of the one- and two-photon absorption spectra is made.

II. METHODS

The method utilized for obtaining statistically averaged values can be divided into two steps: First molecular dynamics (MD) simulations were carried out generating a large number of solute-solvent configurations, and afterwards a CC/MM response calculation was carried out for each configuration.

A. MD simulations

The MD simulations were performed using the MOLSIM program.[40] The simulations were performed within the *NVT* ensemble with the temperature fixed at 25 °C. A cubic simulation box with a length of 24.86 Å containing 512 rigid water molecules was used in order to reproduce the experimental density of water at 25 °C and 1.0 atm of 997.0470 kg/m^3. The intramolecular geometries were $R_{OH}=0.9572$ Å and $\angle_{HOH}=104.49°$, as given in Ref. 41, and for formaldehyde $R_{CO}=1.211$ Å, $R_{CH}=1.100$ Å, $\angle_{OCH}=121.9°$, and $\angle_{HCH}=116.2°$, as given in Ref. 42. The simulations were initiated from a lattice structure, and the system was equilibrated for 300 ps (water/water) and 600 ps (water/formaldehyde) with time steps of 2.0 fs. The potentials used for the simulations are given in Refs. 43–45. In the case of the water/formaldehyde system, one of the 512 water molecules was replaced with a formaldehyde molecule and the system was reequilibrated for 600 ps using the box size for liquid water. The concentration of formaldehyde in this aqueous solution is 0.108 M. After the (re)equilibrations, the simulations were run for 1.5 and 1.2 ns for the water/water and water/formaldehyde systems, respectively, and configurations were dumped every 1 ps giving a total of 1500 (water/water) and 1200 (water/formaldehyde) configurations.

B. CC/MM calculations

The theoretical framework and implementational aspects of the CC/MM method have been presented in previous papers (for electronic excitation energies and linear response properties, see Refs. 46–49). Here, we briefly mention the main characteristics of the CC/MM model. The CC/MM model is a hybrid quantum-classical method where the two subsystems (quantum and classical) are coupled semiclassically. As in most hybrid quantum mechanical/molecular mechanics (QM/MM) methods, the total energy of the system is defined as

Downloaded 08 Nov 2006 to 137.195.101.208. Redistribution subject to AIP license or copyright, see http://jcp.aip.org/jcp/copyright.jsp

TABLE I. Parameters for the potentials used in the QM/MM calculations. The units of α are Å^3, σ's are in Å, while ϵ's are in kJ mol^{-1}.

Potential	q_O	q_H	α	σ_O	σ_H	ϵ_O	ϵ_H
TIP3P	−0.834	0.4170	0.00	3.1507	0.00	0.6362	0.00
SPC-pol 1	−0.669	0.3345	1.44	3.1660	0.00	0.6506	0.00
SPC-pol 2	−0.662	0.3310	1.41	3.1660	0.00	0.6506	0.00

$$E = E_{QM} + E_{QM/MM} + E_{MM}, \tag{1}$$

which implies an analogous separation of the Hamiltonian. The term E_{QM} is the usual quantum mechanical energy described by the many-body vacuum Hamiltonian (QM) and $E_{QM/MM}$ represents the interaction between the QM and MM subsystems. Finally, E_{MM} describes the classically treated portion of the total system. Using a mean-field description of the coupling between the two subsystems,[50,51] we may, according to the theory of intermolecular interactions, decompose the QM/MM energy into different contributions. These contributions account for electrostatic interactions, dispersion and short-range interactions, and polarization of the MM system by the QM system and vice versa. The electrostatic interactions are modeled by assigning partial point charges to the MM nuclei (the q values in Table I), which are introduced into the one-electron part of the many-body vacuum Hamiltonian. Dispersion and short-range effects are, as in most hybrid QM/MM methods, described by the introduction of a potential independent of the QM electronic degrees of freedom (the approach taken in the present work). Alternatively, direct methods have been proposed in which dispersion is accounted for directly in the optimization of the electronic wave function.[50,52] Finally, polarization effects are introduced semiclassically using the QM/MM polarization Hamiltonian,

$$\hat{H}^{pol} = -\frac{1}{2}\sum_{a=1}^{A} \boldsymbol{\mu}_a^{ind}\{\hat{\boldsymbol{R}}\boldsymbol{r}_a + \mathbf{E}^n(\mathbf{R}_a)\}, \tag{2}$$

where $\boldsymbol{\mu}_a^{ind}$ is the induced dipole moment at the center a, $\hat{\boldsymbol{R}}\boldsymbol{r}_a$ is the QM electronic electric field operator, $\mathbf{E}^n(\mathbf{R}_a)$ is the QM nuclear electric field at the center a, and $\mathbf{R}_a$ is the vector from origin to the center of mass of the ath MM molecule. In a linear approximation (and neglecting contributions of magnetic character), $\boldsymbol{\mu}_a^{ind}$ is related to the total electric field at the center a as

$$\boldsymbol{\mu}_a^{ind} = \boldsymbol{\alpha}_a \mathbf{E}_a^{tot}, \tag{3}$$

where $\boldsymbol{\alpha}_a$ is the electric dipole-dipole polarizability at the center a (see Table I). Insertion of Eq. (3) into Eq. (2) allows for a determination of the effective operator accounting for the polarization effects. We note that this treatment of polarization effects includes all terms linear in $\boldsymbol{\alpha}_a$ and, thereby, the relaxation of the induced moments due to an external perturbation. For a detailed discussion of this issue, we refer to Ref. 46. The electric dipole-dipole polarizability in Eq. (3) is approximated by the frequency-independent electric dipole-dipole polarizability. Because our intent is to make a comparison between a CC description (excluding all vibrational contributions) and a CC/MM description of the system, the electric dipole-dipole polarizability includes only the purely electronic contribution, i.e., $\boldsymbol{\alpha}_a = \boldsymbol{\alpha}_a^{el}$. Introducing the effects of vibrations on the specific properties would lead to the added inclusion of the vibrational contribution in the electric dipole-dipole polarizability.

The above-discussed interaction terms may be introduced into the time-dependent CC quasienergy Lagrangian, and, following the method outlined in Ref. 37, the linear and higher-order response functions are derived. A pole analysis of the CC/MM linear response function yields expressions for excitation energies, where, in the CC and CC/MM methods, the eigenvalues of the CC Jacobian define the electronic excitation energies. For a detailed discussion, we refer to Refs. 46 and 50.

The transition moments $M_{f\leftarrow g}^{\alpha\beta}(\omega)$ for n-photon excitations have been defined in a seminal work by Meath and Power.[53] In the case of a two-photon absorption of two photons with identical energy, the resulting transition moments are given as

$$M_{f\leftarrow g}^{\alpha\beta}(\omega) = \sum_i \frac{\langle\Psi_g|\mu_\alpha|\Psi_i\rangle\langle\Psi_i|\mu_\beta|\Psi_f\rangle}{\omega_i - \omega} + \frac{\langle\Psi_g|\mu_\beta|\Psi_i\rangle\langle\Psi_i|\mu_\alpha|\Psi_f\rangle}{\omega_i - \omega}, \tag{4}$$

$$M_{f\leftarrow g}^{\alpha\beta}(\omega)^* = M_{g\leftarrow f}^{\alpha\beta}(-\omega). \tag{5}$$

In Eq. (4) Ψ_f, Ψ_i, and Ψ_g are the wave functions for the final, intermediate, and ground states, respectively, ω_i is the transition energy from the ground state to the intermediate state, ω is the energy that corresponds to the specific laser frequency used to probe the molecule, and μ_α and μ_β are the α and β components (respectively) of the dipole moment operators, where α and β denote the Cartesian coordinate axes x, y, or z. In the present work, we have described the two-photon transition with laser energies equal to half the energy of the state being investigated. In exact state response theory, or for a variational wave function with an orthonormal parametrization of the bra and ket states, the two-photon transition moments are real $[M_{f\leftarrow g}^{\alpha\beta}(\omega)^* = M_{f\leftarrow g}^{\alpha\beta}(\omega)]$. However, this is not the case for coupled-cluster theory as a biorthonormal parametrization is used and the transition moments $M_{f\leftarrow g}^{\alpha\beta}(\omega)$ and $M_{g\leftarrow f}^{\alpha\beta}(-\omega)$ are thus not each others' complex conjugate. Therefore one instead works with the symmetrized two-photon transition strengths defined below.[54,55] The coupled-cluster two-photon transition moments have been derived by Hättig *et al.*[55] from the first residue of the quadratic response function. However, it is typically the two-photon absorption cross section $\sigma(\omega)$ that is measured and this property is given as[56]

Downloaded 08 Nov 2006 to 137.195.101.208. Redistribution subject to AIP license or copyright, see http://jcp.aip.org/jcp/copyright.jsp

$$\sigma(\omega) = \frac{\pi^2 e^4}{c^2 \epsilon_0^2 h^2} \omega^2 g(2\omega) \left(\frac{1}{30} \sum_{\alpha,\beta} (2M^{\alpha\alpha}_{f\leftarrow g}(\omega) M^{\beta\beta}_{f\leftarrow g}(\omega)^* + 4M^{\alpha\beta}_{f\leftarrow g}(\omega) M^{\beta\alpha}_{f\leftarrow g}(\omega)^*) \right), \quad (6)$$

where the normalized function $g(2\omega)$ is the line shape function of the transition. The line shape function is difficult to determine, and instead the sum of the product of transition moments, $\delta(\omega)$, defined as (for linear parallel polarized light beams)

$$\delta(\omega) = \frac{1}{30} \sum_{\alpha,\beta} 2M^{\alpha\alpha}_{f\leftarrow g}(\omega) M^{\beta\beta}_{f\leftarrow g}(\omega)^* + 4M^{\alpha\beta}_{f\leftarrow g}(\omega) M^{\beta\alpha}_{f\leftarrow g}(\omega)^*, \quad (7)$$

denoted as the two-photon transition strength, will be used in the following for comparing the calculated two-photon absorption data. Using this parameter, we can simplify the expression for $\sigma(\omega)$,

$$\sigma(\omega) = 4\pi^2 \alpha^2 \omega^2 g(2\omega) \delta(\omega), \quad (8)$$

where α is the fine structure constant. The $\delta(\omega)$ values presented will be in atomic units. The conversion between a.u. to *Systeme International* (SI) units is 1 a.u.$=m_e^2 a_0^8/\hbar^4$.

In the initial calculations performed on microsolvated formaldehyde, we used three different potentials for describing the interactions between the solvent and the solute, resulting in different forms of the $\hat{H}_{\mathrm{QM/MM}}$ operator. Simple point charge models were used (SPC-pol 1 and 2 and TIP3P), where each atom in the solvent is assigned a charge. Furthermore, in two of the models (SPC-pol 1 and 2), each solvent molecule is further assigned a polarizability. The partial charges and the polarizabilities used in each of the models are presented in Table I.

All computations were performed using the DALTON program[57] interfaced with the MIDAS vibrational structure program[58] to perform the statistical averaging of the molecular properties.

III. RESULTS AND DISCUSSION

In the following, we first consider microsolvation of formaldehyde and formaldehyde-water aggregates immersed in a number of rigid MM water molecules. Following these are results of TPA cross sections calculated by including a significant number (approximately 140–160), described with molecular mechanics, of water molecules around the solute (i.e., increasing the size of the quantum mechanically treated aggregate as well as the number of solvent molecules). Finally, we detail the results for liquid water in which one water was treated quantum mechanically while the others were treated with MM.

A. Microsolvated formaldehyde ($n\rightarrow\pi^*$ transition)

Excitation energies and TPA cross sections for the $n\rightarrow\pi^*$ transition are presented in Table II for the calculations carried out on the molecular aggregates consisting of formaldehyde and water molecules with geometries determined from B3LYP/cc-pVTZ optimizations (taken from Ref. 42). The 1*s* orbitals on C and O were not included in the calculation of the dynamical electron correlation (frozen core). One, two, and four water molecules were included in the solvent calculations, where the water molecules were treated with either quantum mechanics (with up to three water) or with molecular mechanics. By comparing the theoretical methods used, we see that the CC2 TPA results are twice as large as the CCSD numbers, which is not surprising since the CC2 method is known to overestimate the property in question.[27,59] A solvent shift is observed as we see an increase in the excitation energy and a decrease in the TPA cross section when comparing the gas-phase values with the numbers for the microsolvated structures and is also not crucially dependent of the potential used in the calculations. QM/MM calculations were then carried out on an aggregate consisting of formaldehyde and up to four water molecules at a randomly picked "snapshot" from a MD simulation. Here zero to three water molecules were described using quantum mechanics and the rest with molecular mechanics using the geometry in Table III. The TPA cross sections for the aggregates do not seem to depend much on the number of water molecules described with quantum mechanics (Table IV). We also note that the excitation energy for a single formaldehyde molecule calculated with the two geometries used above (either from Table III or from Ref. 42) deviates by 0.05 eV.

B. Statistically averaged excitation energies and TPA cross sections

Configurations from a molecular dynamics calculation were used to further investigate the solvent shift of the TPA cross section for the $n\rightarrow\pi^*$ transition. The configurations were dumped after every picosecond, and altogether 1200 configurations were used for the QM/MM calculations. The cutoff in the QM/MM simulations was 10 Å which amounts to approximately 140–160 water molecules for each configuration. In all the calculations, the formaldehyde molecule was oriented with the C═O bond along the *z* axis, which is particularly important for the following. Initially, calculations were carried out using the 6-31++G basis set and a frozen core CCSD wave function. We used the SPC-pol 1 potential for the calculation. Calculations where carried out, where we included zero, one, and two water molecules in the quantum mechanical system including for each configuration the water molecules closest to the oxygen atom of formaldehyde. The statistical distribution of the TPA cross sections is presented in Fig. 2 and the average cross sections obtained from these distributions are 0.1059 ± 0.0005, 0.171 ± 0.003, and 0.212 ± 0.004 by including zero, one, and two water molecules, respectively, in the system described with quantum mechanics. Thus the observed skewness of the distribution affects the average value of the cross section.

The distribution for the TPA cross sections is Gaussian when no water molecules are included in the quantum mechanical calculations. When more water molecules are included, we see a more skewed distribution. Interestingly, the same trend is observed for the size of the *z* component of the dipole moment, whereas the distributions for both the *x* and *y* components are Gaussian irrespective of the number of water

Downloaded 08 Nov 2006 to 137.195.101.208. Redistribution subject to AIP license or copyright, see http://jcp.aip.org/jcp/copyright.jsp

TABLE II. Calculated $\delta(\omega)$ values for formaldehyde in water using the CC2 and CCSD models. The water molecules are either described in a full quantum mechanical way or using molecular mechanics. The basis set used was in all cases aug-cc-pVDZ. The 1*s* orbitals on C and O were kept frozen. Excitation energies are in eV and the TPA cross sections in a.u.

System	Method	E_{ex}	ΔE_{ex}	δ_{TPA}	$\Delta\delta_{TPA}$
	One water				
H_2CO+H_2O	CC2	4.26	0.18	0.31	−0.11
	CCSD	4.20	0.19	0.15	−0.04
	CC2/MM (TIP3P)	4.28	0.20	0.29	−0.13
	CCSD/MM (TIP3P)	4.21	0.20	0.14	−0.05
	CC2/MM (SPC-pol 1)	4.25	0.17	0.30	−0.12
	CCSD/MM (SPC-pol 1)	4.18	0.17	0.15	−0.04
	CC2/MM (SPC-pol 2)	4.25	0.17	0.30	−0.12
	CCSD/MM (SPC-pol 2)	4.18	0.17	0.15	−0.04
	Two water				
H_2CO+2H_2O	CC2	4.23	0.15	0.39	−0.03
	CCSD	4.18	0.17	0.19	0.00
	CC2/MM (TIP3P)	4.27	0.19	0.25	−0.17
	CCSD/MM (TIP3P)	4.21	0.20	0.12	−0.05
	CC2/MM (SPC-pol 1)	4.26	0.18	0.26	−0.16
	CCSD/MM (SPC-pol 1)	4.19	0.18	0.13	−0.06
	CC2/MM (SPC-pol 2)	4.26	0.18	0.26	−0.16
	CCSD/MM (SPC-pol 2)	4.19	0.18	0.13	−0.06
	Four water				
H_2CO+4H_2O	CC2	⋯	⋯	⋯	⋯
	CCSD	⋯	⋯	⋯	⋯
	CC2/MM (TIP3P)	4.31	0.23	0.19	−0.23
	CCSD/MM (TIP3P)	4.25	0.24	0.10	−0.09
	CC2/MM (SPC-pol 1)	4.29	0.21	0.20	−0.22
	CCSD/MM (SPC-pol 1)	4.23	0.22	0.10	−0.09
	CC2/MM (SPC-pol 2)	4.29	0.21	0.20	−0.22
	CCSD/MM (SPC-pol 2)	4.23	0.22	0.10	−0.09
H_2CO (vacuum structure)	CC2	4.08	⋯	0.42	⋯
	CCSD	4.01	⋯	0.19	⋯

molecules treated with quantum mechanics. One explanation for this could be charge transfer between the water molecules and formaldehyde. In a previous paper,[60] the radial distribution function between hydrogen on water and the oxygen atom on formaldehyde was presented. A maximum of approximately 2 Å was found for the distribution function, indicating, as one would expect, hydrogen bonds between water and formaldehyde (the sum of the van der Waals radii for hydrogen and oxygen is approximately 2.5 Å). In Fig. 3 the radial distribution function between the carbon atom in formaldehyde and oxygen in water is presented. A maximum of approximately 3.3 Å is observed which is not consistent with a $C\cdots OH_2$ interaction as the sum of van der Waals radii for carbon and oxygen amounts to approximately 3.0–3.2 Å. Thus, possible charge-transfer effects are merely mediated through hydrogen bonding. However, it is also possible that this observed skewness is due to limitations in our theoretical model, inasmuch as the exchange and dispersion components in the QM/MM potential are treated classically. Irrespective of the origin of the observed skewness in the distributions, we opted to describe two water molecules using quantum mechanics in the calculations carried out with a larger basis set.

TABLE III. Geometry of formaldehyde microsolvated by four water molecules (all coordinates in Å). The oxygens of the water molecules are listed in order of increasing distance to the oxygen on the formaldehyde molecule. The geometry is randomly picked from a MD simulation where the rest of the water molecules are not included.

Molecule	Atom	*x*	*y*	*z*
H_2CO	C	0.0000	0.0000	1.2123
	O	0.0000	0.0000	0.0000
	H	−0.9355	0.0000	1.7950
	H	0.9355	0.0000	1.7950
H_2O	O	0.1841	0.9903	−2.5121
	O	−0.0233	−2.3294	−1.4398
	O	−2.6136	0.5333	−1.1102
	O	1.5624	2.6354	1.4460
	H	1.0982	1.1392	−2.7596
	H	0.2315	0.6250	−1.6271
	H	−0.1978	−1.6719	−0.7644
	H	0.9249	−2.4651	−1.4034
	H	−1.6968	0.3386	−0.9090
	H	−2.9474	−0.2710	−1.5108
	H	1.8616	3.5396	1.5549
	H	0.8031	2.7022	0.8649

Downloaded 08 Nov 2006 to 137.195.101.208. Redistribution subject to AIP license or copyright, see http://jcp.aip.org/jcp/copyright.jsp

TABLE IV. Calculated QM/MM $\delta(\omega)$ values for formaldehyde in water using the CCSD model and the SPC-pol 1 potential. The geometry in Table III was used. The 1*s* orbitals on C and O were kept frozen. Excitation energies are in eV and the TPA cross sections in a.u.

System					
QM	MM	E_{ex}	ΔE_{ex}	δ_{TPA}	$\Delta\delta_{TPA}$
H_2CO+0H_2O		3.96	···	0.19	···
H_2CO+0H_2O	$1H_2O$	4.04	0.08	0.14	–0.05
$1H_2O$	$0H_2O$	4.07	0.11	0.14	–0.05
H_2CO+0H_2O	$2H_2O$	4.01	0.05	0.10	–0.09
$1H_2O$	$1H_2O$	4.04	0.00	0.11	–0.08
$2H_2O$	$0H_2O$	4.08	0.12	0.11	–0.08
H_2CO+0H_2O	$3H_2O$	4.14	0.18	0.08	–0.11
$1H_2O$	$2H_2O$	4.17	0.21	0.10	–0.09
$2H_2O$	$1H_2O$	4.20	0.24	0.09	–0.10
$3H_2O$	$0H_2O$	4.18	0.14	0.08	–0.11
H_2CO+0H_2O	$4H_2O$	4.17	0.21	0.08	–0.11
$1H_2O$	$3H_2O$	4.19	0.23	0.10	–0.09
$2H_2O$	$2H_2O$	4.22	0.26	0.08	–0.11
$3H_2O$	$1H_2O$	4.20	0.24	0.07	–0.12

We now turn to the number of configurations needed for obtaining a converged TPA cross section. For these studies we used calculations which were carried out using either the SPC-pol 1 or the TIP3P potential with a CCSD/6-31++G wave function (formaldehyde and two water molecules were described using quantum mechanics). Convergence profiles are presented in Fig. 4. The configurations are included in order that they are dumped from the molecular dynamics simulation, so that, for example, the first ten configurations in the convergence profiles correspond to snapshots of the first 10 ps in the molecular dynamics simulation. Similar convergence profiles are observed for the two potentials used, where the only difference is manifested in the converged values for the TPA cross section. A value of 0.212 ± 0.004 a.u. is obtained for the SPC-pol 1 potential, and 0.206 ± 0.004 a.u. is obtained for the TIP3P potential. Furthermore, we need to include approximately 700 configurations in order to obtain an average value that is converged. However, after 50 configurations, a value is obtained that is quite close to the converged value (within 0.1 a.u.). Our previous gas-phase calculations for the TPA cross sections on formaldehyde[27] revealed that a sufficient basis set for obtaining accurate values is the aug-cc-pVDZ basis set. Presently, it is computationally very demanding to perform 700 CCSD/MM/aug-cc-pVDZ calculations on formaldehyde and two water molecules. Thus we carried out 60 calculations using the CCSD/MM/aug-ccpVDZ wave function (with 1*s* orbitals on C and O frozen) and obtained a value of 0.15 ± 0.01 a.u. for the TPA cross sections of the first excited state of formaldehyde (see Table V). The cross section for a formaldehyde molecule in vacuum is 0.19 a.u., indicating a decrease in the cross section due to solvent effects.

To the best of our knowledge, the present work constitutes the first theoretical report of the solvation effect on the TPA cross section of formaldehyde. For an overview of the solvent effects on the $n\rightarrow\pi^*$ single photon transition in formaldehyde or acetone, we refer to our previous works[60,61] as well as very recent studies by Hirata *et al.*,[62] D'Abramo *et al.*,[63] and Sánchez *et al.*[64]

C. Liquid water

Recently, the CC/MM response methodology has been successfully applied in calculating the excitation energies, transition strengths (oscillator strengths) and polarizability, and first hyperpolarizability of liquid water.[49,51,65,66] The present work constitutes the first attempt to elucidate the effects of solvation on the two-photon absorption cross section of liquid water using the CC/MM approach. Previously, Poulsen *et al.*[19] utilized multiconfigurational self-consistent field (MCSCF)/MM response theory for calculating the solvent effects on TPA of liquid water using an average structure, and in passing we point out our recently performed benchmark calculations of the two-photon absorption of the lowest five excited states of gas-phase water including triples contributions with the CC3 model.[27] These results showed that including triple excitations in the CC wave function only affected the excitation energies and TPA cross section for water by around 5% compared to CCSD results and that the basis set was a much more important issue. A similar conclusion was drawn from recent configuration interaction (CI) investigations,[28] where we included up to pentuple excitations in the wave function for calculating the TPA cross sections. Here triple excitations were necessary to obtain a converged value. However, in the CCSD wave function, the single and double excitations are coupled in the exponential parametrization, thus including the most important effects of higher excitations in the wave function.

For an accurate description of the TPA cross section of a single water molecule (gas phase), it was necessary to use a doubly augmented basis set, and the smallest possible basis which gave reasonably reliable results was the *d*-aug-cc-pVDZ basis. This basis set was therefore used in all calculations discussed below.

In our studies on the two-photon absorption of liquid water, we have used a similar strategy to that used above for formaldehyde, except that we have used a total of 1500 configurations. Similar to the formaldehyde simulations, a cutoff radius in the CC/MM calculations of 10 Å was used. The larger number of configurations in this case was in part due to the slower convergence of the TPA cross section and will be discussed in more detail below. We initially compared QM/MM results for the TPA cross section of a water pentamer (C_{2v} symmetry) with fully quantum mechanical calculations similar to the approach used for formaldehyde above. The pentamer was constructed such that one central water molecule is surrounded by four water molecules with an O···H distance matching the maximum in the experimental O···H radial distribution function. For details about the ge-

Downloaded 08 Nov 2006 to 137.195.101.208. Redistribution subject to AIP license or copyright, see http://jcp.aip.org/jcp/copyright.jsp

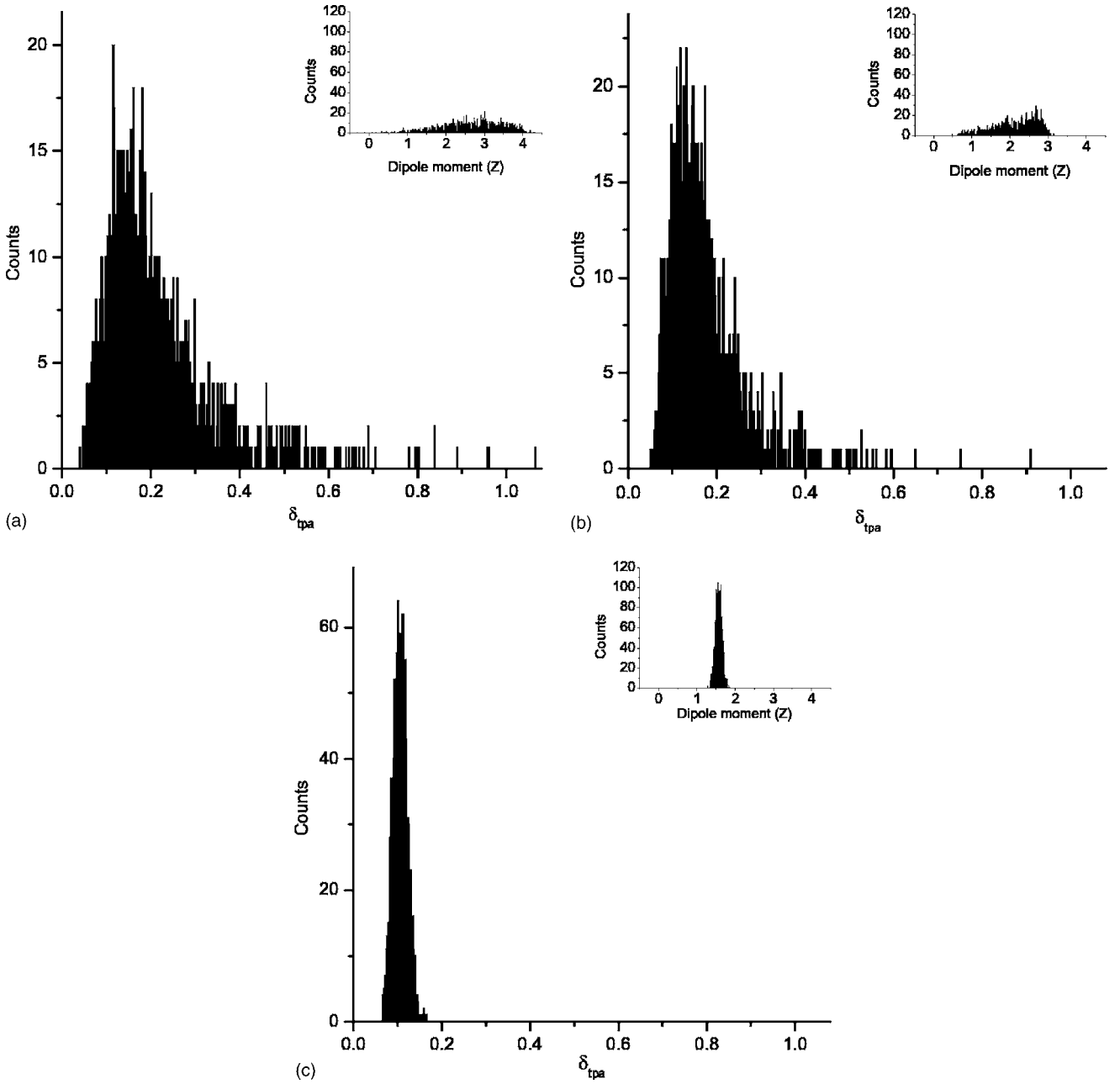

FIG. 2. Statistical distributions of δ [Eq. (7)] with two (a), one (b), and zero (c) water molecules in the aggregate described with quantum mechanics. The inserts show the distribution of the dipole moment in the z direction.

ometry used, see Ref. 67. The results for the CCSD/d-aug-cc-pVDZ response calculations for the lowest five states of the pentamer in C_{2v} symmetry are presented in Table VI. Also listed are the results for the pentamer calculations with only one water molecule treated using CCSD/d-aug-cc-pVDZ and the rest treated with either the TIP3P or the SPC-pol 1 potentials. The comparison between CCSD and CCSD/MM is only valid for states localized on the central water molecule of the pentamer, i.e., one is not interested in pentamer results but rather a single water molecule solvated by four other water molecules.

The determination of which states correlate with the central water molecule is a nontrivial task but has been carried out in Ref. 67 in which the monomer excited states were correlated adiabatically with those of the pentamer by removing the four surrounding water molecules to infinity. It was found that in an idealized C_{2v} geometry, the lowest excited state of $^1B_1$ symmetry can be separated from the others as the excitation on the central water molecule correlating to the first excited state of the water monomer. We have therefore used this state in our comparison of the CCSD/MM model with the full quantum mechanical calculations. From Table VI it is clear that both the excitation energy and TPA cross section compare favorably with the CCSD results of the pentamer. We note that the TIP3P potential gives fortuitously better agreement with full CCSD than the superior SPC-pol 1 potential but that generally both the excitation energies and TPA cross sections are in fairly good agreement.

Downloaded 08 Nov 2006 to 137.195.101.208. Redistribution subject to AIP license or copyright, see http://jcp.aip.org/jcp/copyright.jsp

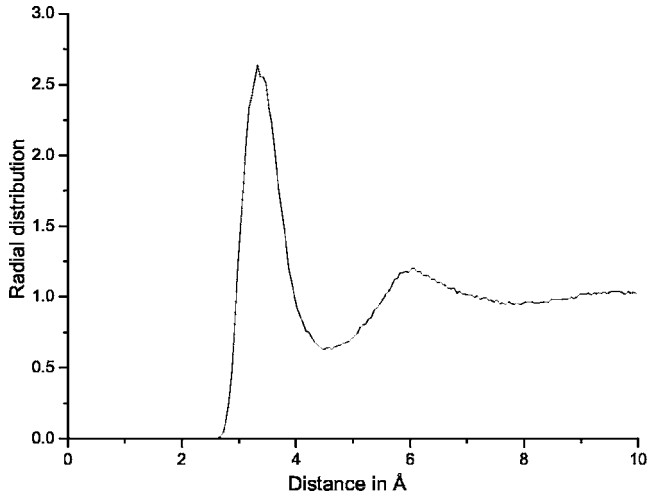

FIG. 3. Radial distribution function for the distance between C on formaldehyde and O on water generated from simulations with the SPC-pol 1 force field.

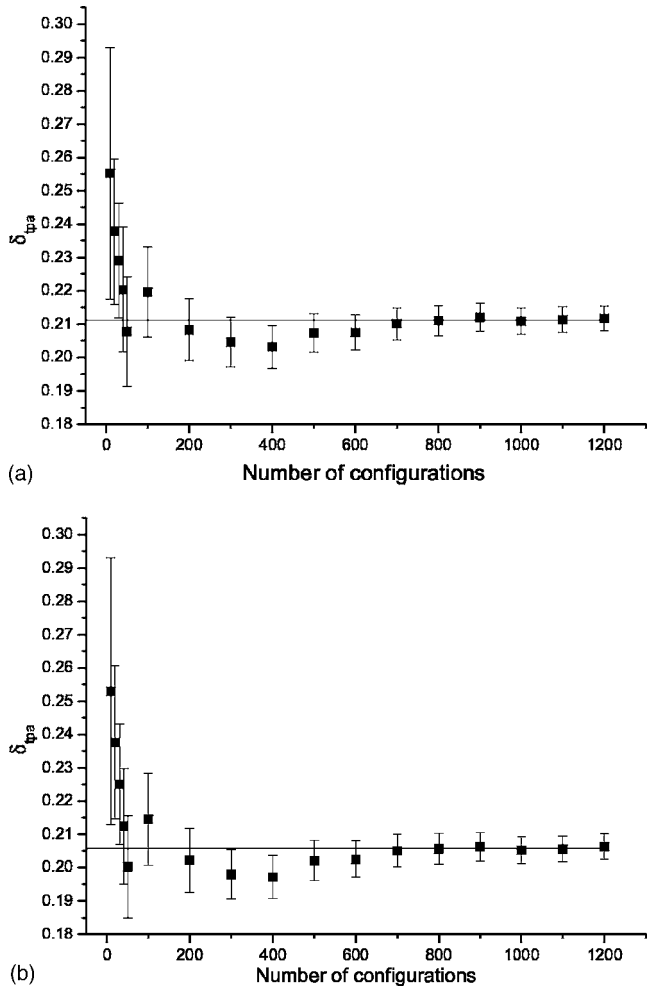

FIG. 4. δ [Eq. (7)] as a function of the number of configurations included in the statistical averaging using either the SPC-pol 1 potential (a) or the TIP3P potential (b) with a CCSD/6-31++G wave function. The error bars are calculated according to $\sigma/\sqrt{N}$. The horizontal lines indicate the values for the TPA cross section obtained using 1200 solute-solvent configurations.

TABLE V. Calculated $\delta(\omega)$ values for formaldehyde and two water in water using the CCSD model. The basis set used was aug-cc-pVDZ. The 1*s* orbitals on C and O were kept frozen. Excitation energies are in eV and the TPA cross sections in a.u.

Configurations	E_{ex}	ΔE_{ex}	δ_{TPA}	$\Delta\delta_{TPA}$
10	4.28±0.03	0.27±0.03	0.16±0.03	−0.03±0.03
20	4.32±0.02	0.31±0.02	0.15±0.02	−0.04±0.02
30	4.33±0.02	0.31±0.02	0.15±0.01	−0.04±0.01
40	4.35±0.02	0.34±0.02	0.14±0.01	−0.05±0.01
50	4.34±0.01	0.33±0.01	0.15±0.01	−0.04±0.01
60	4.33±0.01	0.31±0.01	0.15±0.01	−0.04±0.01

While it would be desirable to also have such comparison as the one just described for the higher excited states, this is a virtually impossible task. In the CCSD/MM calculations the second excited state appears at 9.45 eV, while in the fully quantum mechanical pentamer calculations there are many states (around 20 per symmetry class) below this level. Together with the rather diffuse character of the higher excited states, this makes a safe correlation between monomer states and pentamer states problematic. Therefore, we cannot rigorously validate the approach explicitly for the higher excited states but must be satisfied with observing that the CCSD/MM model with the *d*-aug-cc-pVDZ basis set provides an accurate description (of the TPA cross section) for the lowest excited state.

Figure 5 shows the convergence of the excitation energies of the five lowest excited states, while Fig. 6 shows convergence of the TPA cross section, with respect to the number of configurations sampled. The error bars indicate the standard deviation of the mean value computed at each of the configuration numbers, which were obtained by starting with 1500 configurations from the MD run and removing 100 from the end point each time. In this way all configurations up to each end point are temporally related (according to the original MD run). Although all alternative ways of generating each configuration number should average to the same result, they may individually show different extrema of the average value. This is particularly apparent from the raw data plotted in Fig. 7 for all configurations for the excitation energy and TPA cross section. It can be seen that while the excitation energy oscillates in a relatively well behaved manner around the mean value, the TPA cross section has some dramatic fluctuations which would clearly affect the average if those particular extreme values are included. It is clear that

TABLE VI. Excitation energies (in eV) and TPA cross sections (in a.u.) for a water pentamer using the CCSD wavefunction and the *d*-aug-cc-pVDZ basis set. The 1*s* orbital on O was kept frozen.

	Aggregate (QM)		TIP3P (QM/MM)		SPC-pol 1 (QM/MM)	
State	E_{ex}	δ_{TPA}	E_{ex}	δ_{TPA}	E_{ex}	δ_{TPA}
$^1B_1$	8.11	2.11	8.12	3.72	8.23	4.51
2nd Excited state			9.45	29.87	9.59	26.13

Downloaded 08 Nov 2006 to 137.195.101.208. Redistribution subject to AIP license or copyright, see http://jcp.aip.org/jcp/copyright.jsp

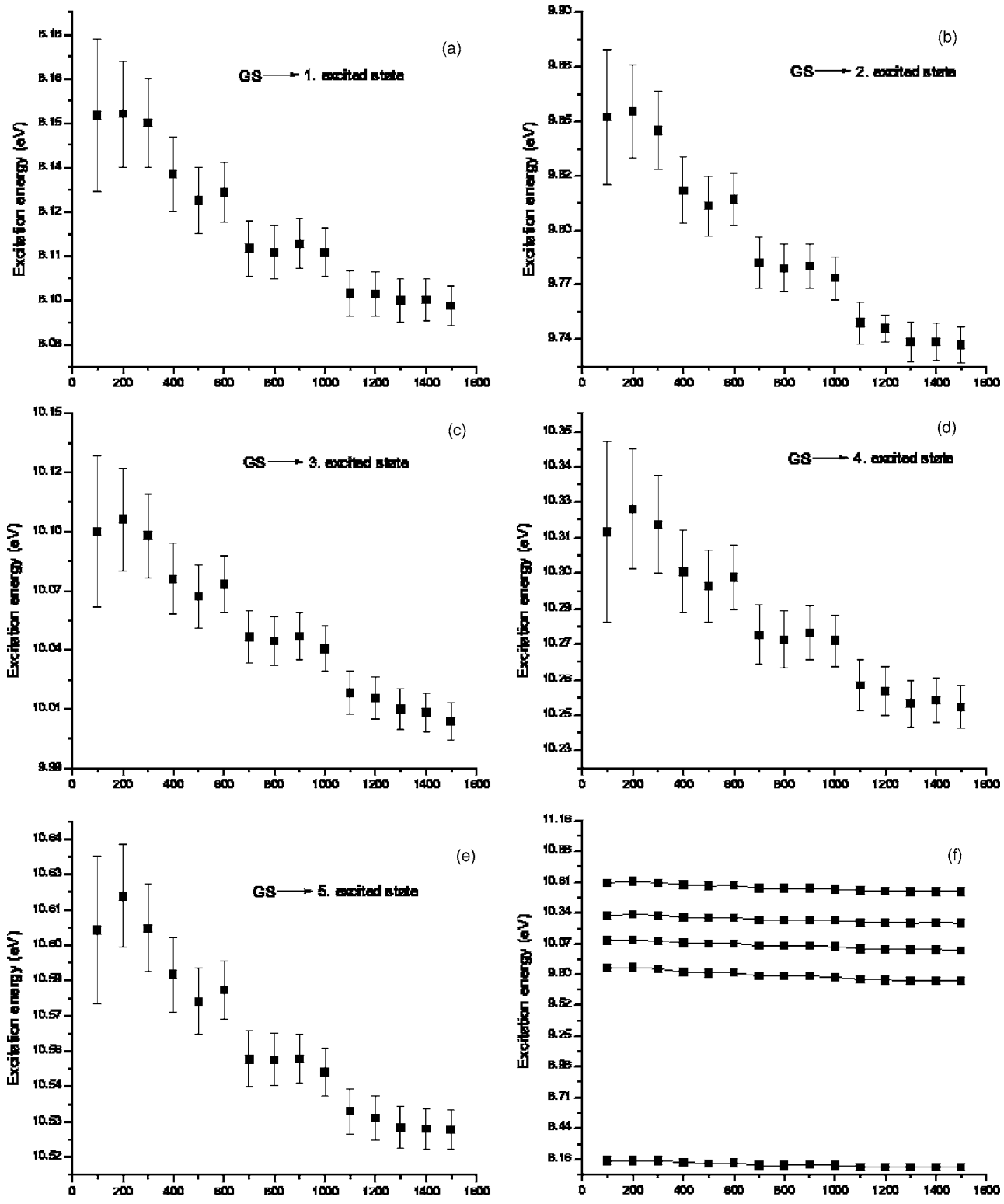

FIG. 5. The excitation energies (in eV) as a function of the number of configurations included in the statistical averaging using the SPC-pol 1 potential with a CCSD/*d*-aug-cc-pVDZ wave function. The error bars are calculated according to $\sigma/\sqrt{N}$.

the convergence of the TPA cross section for water is much poorer than for formaldehyde (compare Figs. 4 and 6). However, one can see that the relative convergence for the five states [Fig. 6(f)] shows that for both the excitation energies and TPA cross sections, the values are almost constant across a range of configurations. Thus, on a relative scale, the effect of the fluctuations (Fig. 7) on the average value is actually modest. Although the convergence is not as nice as for formaldehyde, we nevertheless observe a convergence of both excitation energy and TPA cross section with about 1000 configurations.

From Table VII we see that one solvent effect is an increase in the TPA cross sections for the four lowest states, whereas the cross section for the fifth state is decreased upon

Downloaded 08 Nov 2006 to 137.195.101.208. Redistribution subject to AIP license or copyright, see http://jcp.aip.org/jcp/copyright.jsp

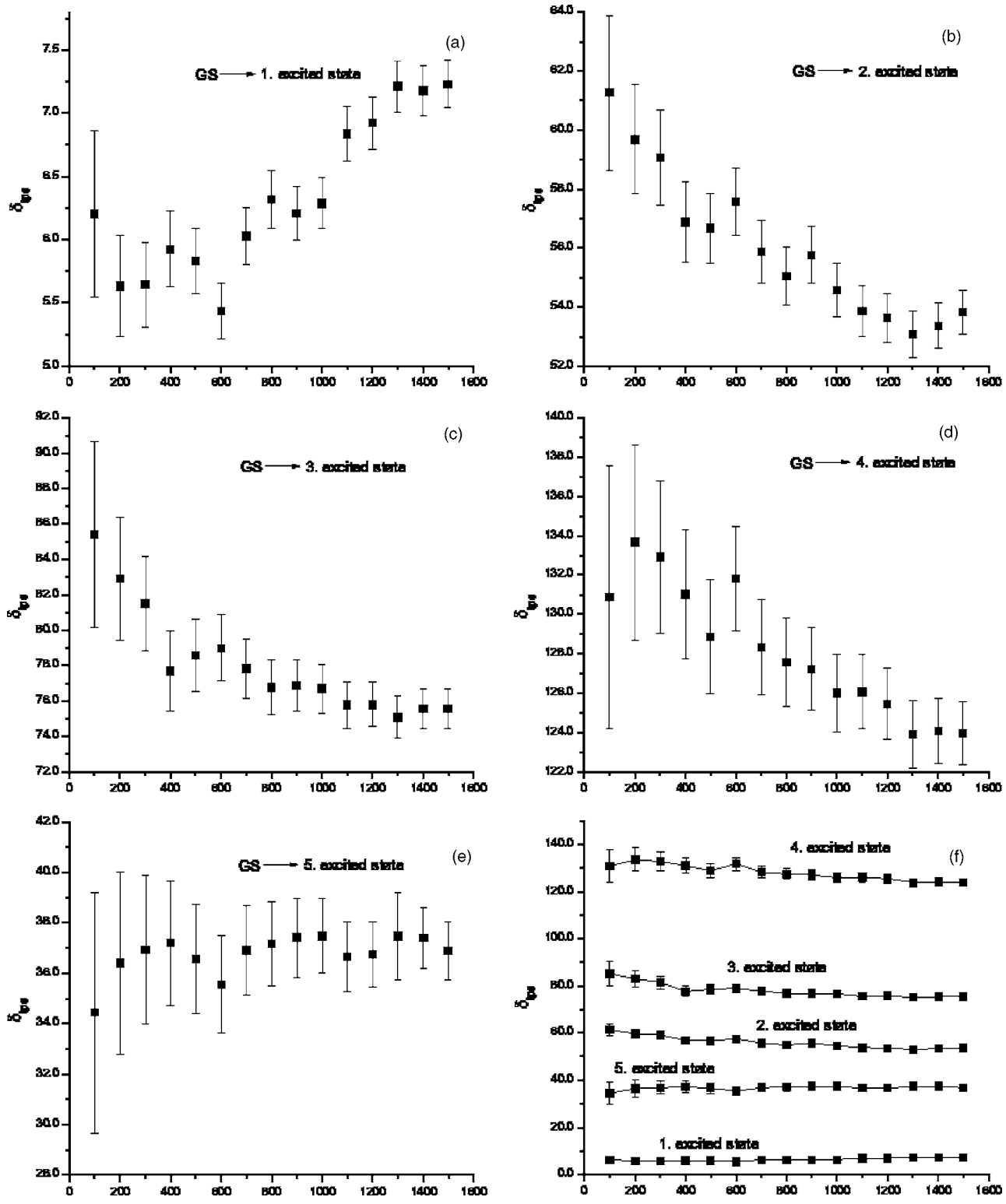

FIG. 6. δ [Eq. (7)] as a function of the number of configurations included in the statistical averaging using the SPC-pol 1 potential with a CCSD/*d*-aug-cc-pVDZ wave function. The error bars are calculated according to $\sigma/\sqrt{N}$.

solvation. It is also for the fifth state that we observe the largest solvent effect. For all the states, the excitation energies are blueshifted upon solvation.

D. Comparison of calculated and experimental absorption spectra for water

The one- and two-photon absorption spectra based on the five lowest excited electronic states are shown in Fig. 8. The spectra are obtained by phenomenologically broadening each excitation, for each configuration, with a Gaussian and "adding them up." The transition strength for each individual excitation was multiplied with either the corresponding energy (one-photon spectrum) or the square of that energy (the two-photon spectrum). The integral of each Gaussian is then made proportional to this cross-section measure with the width of the Gaussian as a parameter. The Gaussian broad-

Downloaded 08 Nov 2006 to 137.195.101.208. Redistribution subject to AIP license or copyright, see http://jcp.aip.org/jcp/copyright.jsp

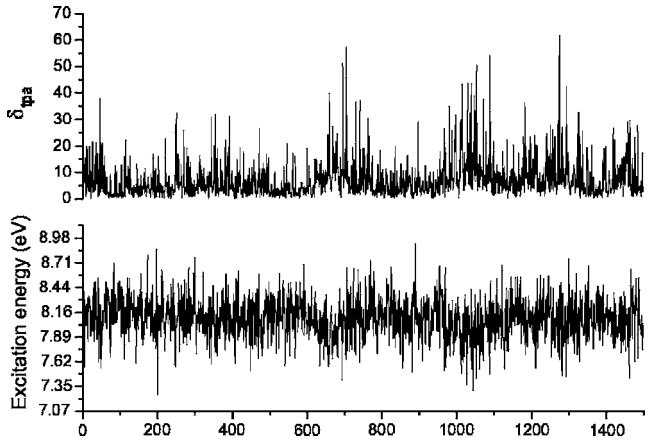

FIG. 7. Liquid water excitation energy and corresponding δ [Eq. (7)] for the lowest excited state with respect to each configuration dumped from the initial molecular dynamics simulation.

ening is used here to provide a measure of broadening. Again, the situation is simplest for the lowest state where excitation to the lowest excited singlet state, causing direct dissociation on an excited state surface, is close to linear around the ground state equilibrium geometry. Correspondingly, already in gas phase the lowest excited singlet state therefore has an absorption spectrum that is close to a Gaussian. For the higher excited states, the picture is more mixed and a simple Gaussian does not in a fair way account for the varied dynamics taking place.[68] However, in this study of the solvent effects on the excitation we do not want to enter into too much detail concerning this subject and we have opted for the simplest approach of using one common full width at half maximum (FWHM) for all states leaving only one parameter in converting the large set of numbers for different configurations and states into a single spectrum.

Two experimental TPA spectra are included for comparison. One of the spectra originates from Ref. 23, where two-photon absorption coefficients were measured at five different wavelengths. These were then converted to TPA cross sections in Ref. 28. The TPA spectrum covering the broadest spectral range originates from Ref. 22, and it is important to note that this spectrum is a relative spectrum scaled to fit within the range of the absolute cross sections obtained from Ref. 23. Moreover, this relative spectrum was recorded by using one fixed laser frequency (266 nm) and varying the other laser frequency. Thus the two-photon excitation does not occur by absorbing two photons with the same energy as is the case with the experimental values from Ref. 23.

The width of the Gaussian clearly has an effect on the appearance of the spectrum: 0.1 eV giving spectra too defined but 0.9 eV being too broad. For a FWHM of about

TABLE VII. Comparison of gas-phase (data from Ref. 27) and condensed-phase TPA excitation energies (eV) and TPA cross sections (a.u.) obtained from CCSD/*d*-aug-cc-pVDZ calculations. Condensed-phase results are averaged over 1500 configurations. The gas-phase data in parentheses are results from CC3/*d*-aug-cc-pVQZ calculations (see Ref. 27).

	Vacuum		Liquid-phase	
State	E_{ex}	δ_{TPA}	E_{ex}	δ_{TPA}
1	7.43(7.66)	4.98(4.74)	8.094±0.006	7.2±0.2
2	9.18(9.42)	46.41(40.64)	9.739±0.009	53.8±0.8
3	9.72(9.83)	67.45(35.44)	10.008±0.008	76±1
4	9.81(10.10)	45.41(39.69)	10.248±0.008	124±2
5	10.04(10.28)	200.09(223.64)	10.528±0.007	37±1

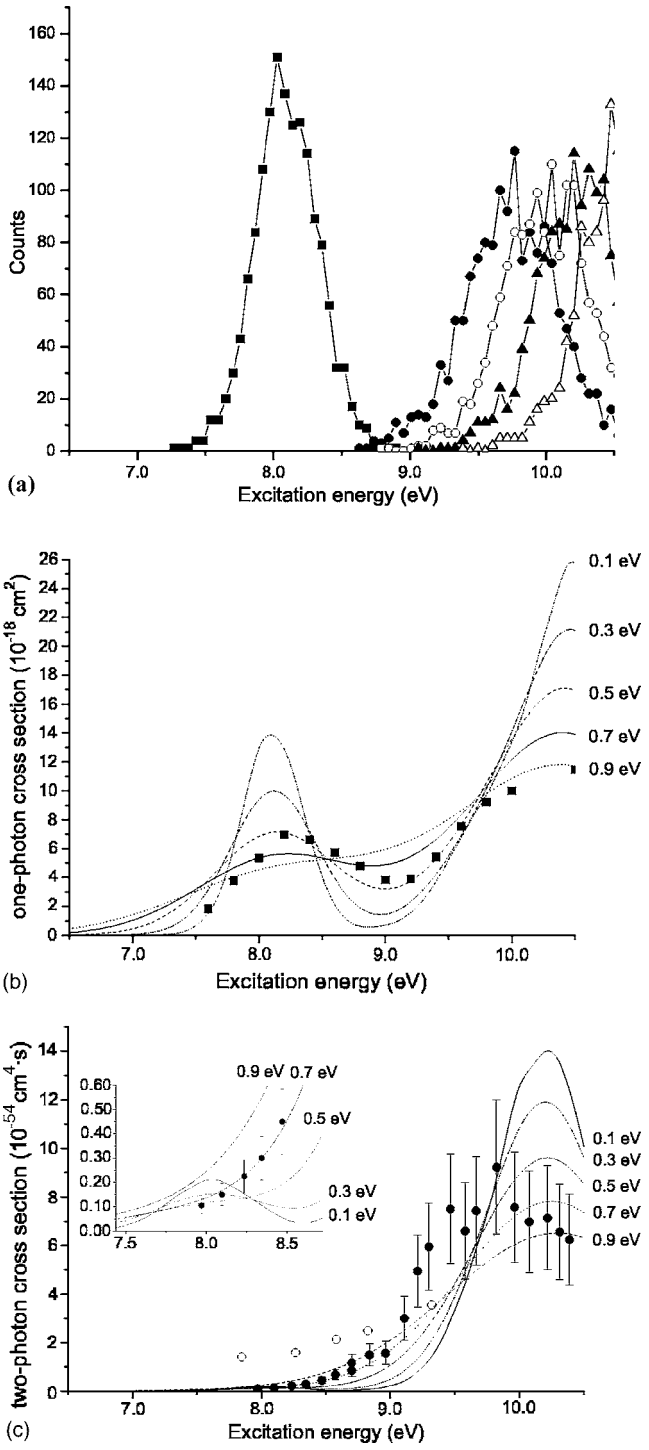

FIG. 8. Frequency count of the excitation energies sampled in 0.05 eV intervals (a). Calculated liquid water one- (b) and two-photon (c) absorption spectra (relative values) from the lowest five excitations. Phenomenological broadening of 0.1, 0.3, 0.5, 0.7, and 0.9 eV of the calculated transitions is considered. For comparison experimental TPA spectra from Refs. 23 (open circles) and 22 (closed circles) are included. It is only the cross section from Ref. 23 that is absolute. All other TPA data are relative values. The experimental one-photon spectrum (filled squares) was taken from Ref. 69.

Downloaded 08 Nov 2006 to 137.195.101.208. Redistribution subject to AIP license or copyright, see http://jcp.aip.org/jcp/copyright.jsp

0.5 eV, both the one-photon absorption (OPA) and TPA spectra compare well with experiment.[22] In the experimental spectra, the second band (occurring at approximately 10 eV) is twice as intense as the first band (occurring at approximately 8 eV) in the one-photon absorption spectrum[69] and much more dominant for TPA. Indeed we observe that essentially all the spectral features in the experimental one- and two-photon absorption spectra of water in the condensed phase are reproduced including the relative intensities of the first two bands (in arbitrary units). However, the calculated TPA spectrum appears to be blueshifted by approximately 0.5 eV in comparison with the experimental spectrum, obtained from Ref. 22. One of the main effects of solvation on the two-photon absorption spectrum is a relative decrease in the intensity of the first band and an increase in the intensity of the second band, relative to the gas-phase results, and an accompanying spectral shift to the blue.[27] This finding is particularly important for the interpretation of two-photon absorption spectra. It has often been expected (and observed) that the two-photon absorption spectrum has a similar spectral profile to the one-photon absorption spectrum unless the molecule has an inversion center. In that case, selection rules dictate a difference as gerade-gerade and ungerade-ungerade transitions are forbidden in a one-photon excitation scheme but allowed in a two-photon excitation process, and gerade-ungerade transitions are allowed in a one-photon excitation process but forbidden in a two-photon excitation process.[56] However, in water there is no inversion center and, in fact, the transitions occurring at approximately 8 eV in the one-photon absorption spectrum are relatively weak in the two-photon absorption spectrum. This interpretation is in agreement with experimental results, previous estimates based on gas-phase calculations,[27] and now also confirmed by our condensed-phase calculations.

One caveat must be kept in mind, however, when considering the theoretical modeling of the water excitation spectra: The gas-phase excited states are known to have primarily Rydberg character and what happens to these states in the condensed phase is a complex problem.[67,70,71] In solution the diffuse Rydberg states would overlap significantly with the orbitals of solvent molecules and accurate modeling of such effects can be expected to require the inclusion of the solute-solvent exchange component in the QM/MM interaction operator or by considering an aggregate consisting of several water molecules as the QM system in the QM/MM calculations. The latter option is of course not free from border effects and is very complicated as mentioned above (see also Ref. 67). Deriving a convenient and accurate operator for the first option is also highly challenging. For these reasons it is noteworthy that our simple QM/MM approach is capable of reproducing the experimental features rather well. This agreement is ascribed to an optimal choice of model parameters which compensates for some of the physical interactions that are not described with the QM/MM model operator (e.g., no operators are included in the QM/MM operator to describe solute-solvent exchange).

We have previously calculated and analyzed the single photon excitation spectrum of liquid water using the CC/MM method combined with the *d*-aug-cc-pVDZ basis set and obtained a location of the lowest transition around 8.3 eV (Ref. 49) which compared well with the corresponding result obtained in the present study (8.094±0.006 eV) using the *d*-aug-cc-pVDZ basis set. An experimental value of 8.4 eV has been reported,[72] but more recent experiments[22,69,71] suggest an experimental value of 8.2 eV in favor of our theoretical predictions. Very recently, Aschi *et al.*[73] have performed calculations of the single photon excitation spectrum using the perturbed matrix method (PMM) and obtained excitation energies of 8.3 and 8.5 eV using a CC and complete active space self-consistent field (CASSCF) wave function, respectively. The result based on the CC approach is in very good agreement with our findings while the CASSCF is seen to lead to slightly overestimated results. As noted in Ref. 73 the TAB/10D calculations from Bursulaya *et al.*[74] agree well with the results based on coupled-cluster methods.

Another useful measure of solvent effects is the solvent shift, that is, the change in excitation energy for a transition in vacuum in comparison to the liquid state. Using experimental values[22,69,71] of 8.2 and 7.4 eV (Ref. 75) for the lowest energy transitions occurring in the liquid and vapor phase excitation spectra, respectively, we obtain a solvent shift 0.8 eV (77 kJ mol^{-1}). This is in reasonably good agreement with our predicted value of 0.66 eV (64 kJ mol^{-1}). A theoretical value of 78 kJ mol^{-1} was reported in Ref. 73 obtained with a CASSCF wave function using statistical averaging based on SPC models. Thus, even though CASSCF leads to underestimated excitation energies, a solvent shift close to the experimental value was obtained.

IV. CONCLUSION

In the present work we have modeled the solvent effect on the TPA cross section for two small molecules, formaldehyde and water, solvated in water. Formaldehyde is the smallest molecule containing a carbonyl group, and the solvent effect on molecules containing carbonyl groups is of importance for research on donor-acceptor molecules with large TPA cross sections. Water is a molecule that forms strong hydrogen bonds, and studying water as a solute solvated in water is thus a probe for the effect of hydrogen bonds on the TPA cross section. Two opposite solvent effects were found: The TPA cross section for the four lowest states of water increased upon solvation in water and decreased for the fifth state, whereas for formaldehyde the cross section for the first excited state decreased. Furthermore, we found that it is necessary to include a number of water molecules in the quantum mechanical system for accurately describing the solvent effects on formaldehyde due to the hydrogen bonds between formaldehyde and water resulting in charge-transfer effects. These effects were seen from the distributions of both the TPA cross sections and the one-photon transition moments.

As formaldehyde dissolved in water is converted to its hydrate, no experimental data are available for comparison. However, for liquid water, we investigated in more detail the one- and two-photon absorption spectra and compared those to available experimental data. No inversion symmetry is present in the water molecule and we thus might *a priori*

Downloaded 08 Nov 2006 to 137.195.101.208. Redistribution subject to AIP license or copyright, see http://jcp.aip.org/jcp/copyright.jsp

expect that the spectral profiles for the one- and two-photon spectra could be similar but this is not observed in the experimental data, and we were able to successfully model this effect, reproducing all experimental spectral features with our simulations.

ACKNOWLEDGMENTS

One of the authors (O.C.) acknowledges support from the Danish National Research Foundation, the Danish Research Agency (SNF), and Danish Center for Scientific Computing (DCSC). Another author (K.V.M.) thanks SNF, DCSC, and the EU network NANOQUANT for support.

[1] P. Cronstrand, Y. Luo, and H. Ågren, Chem. Phys. Lett. **352**, 262 (2002).
[2] P. Cronstrand, Y. Luo, and H. Ågren, J. Chem. Phys. **117**, 11102 (2002).
[3] P. Cronstrand, P. Normann, Y. Luo, and H. Ågren, J. Chem. Phys. **121**, 2020 (2004).
[4] T. D. Poulsen, P. K. Frederiksen, M. Jørgensen, K. V. Mikkelsen, and P. R. Ogilby, J. Phys. Chem. A **105**, 11488 (2001).
[5] S. J. K. Pond, M. Rumi, M. D. Levin, T. C. Parker, D. Beljonne, M. W. Day, J.-L. Brédas, S. R. Marder, and J. W. Perry, J. Phys. Chem. A **106**, 11470 (2002).
[6] M. Rumi, J. E. Ehrlich, A. A. Heikal *et al.*, J. Am. Chem. Soc. **122**, 9500 (2000).
[7] K. D. Belfield, Y. Liu, R. A. Negres, M. Fan, G. Pan, D. J. Hagan, and F. E. Hernandez, Chem. Mater. **14**, 3663 (2002).
[8] W. Denk, J. H. Strickler, and W. W. Webb, Science **248**, 73 (1990).
[9] R. M. Williams, D. W. Piston, and W. W. Webb, FASEB J. **8**, 804 (1994).
[10] G. S. He, P. P. Markowicz, T. C. Lin, and P. N. Prasad, Nature (London) **415**, 767 (2002).
[11] B. A. Reinhardt, L. L. Brott, S. J. Clarson, A. G. Dillard, J. C. Bhatt, R. Kannan, L. X. Yuan, G. S. He, and P. N. Prasad, Chem. Mater. **10**, 1863 (1998).
[12] T. Watanabe, M. Akiyama, K. Totani, S. M. Kuebler, F. Stellacci, W. Wenseleers, K. Braun, S. R. Marder, and J. W. Perry, Adv. Funct. Mater. **12**, 611 (2002).
[13] K. D. Belfield, X. Ren, D. J. Hagan, E. W. Van Stryland, V. Dubikovsky, and E. J. Miesak, Abstr. Pap. - Am. Chem. Soc. **218**, U629 (1999).
[14] B. H. Cumpston, S. P. Ananthavel, S. Barlow *et al.*, Nature (London) **398**, 51 (1999).
[15] G. S. He and P. N. Prasad, J. Opt. Soc. Am. B **15**, 1078 (1998).
[16] G. S. He, N. Cheng, P. N. Prasad, D. Liu, and S. H. Liu, J. Opt. Soc. Am. B **15**, 1086 (1998).
[17] U. Narang, C. F. Zhao, J. D. Bhawalkar, F. V. Bright, and P. N. Prasad, J. Phys. Chem. **100**, 4521 (1996).
[18] T. J. Dougherty, C. J. Gomer, B. W. Henderson, G. Jori, D. Kessel, M. Korbelik, J. Moan, and Q. Peng, J. Natl. Cancer Inst. **90**, 889 (1998).
[19] T. D. Poulsen, P. R. Ogilby, and K. V. Mikkelsen, J. Chem. Phys. **115**, 7843 (2001).
[20] M. Albota, D. Beljonne, J.-L. Brédas *et al.*, Science **281**, 1653 (1998).
[21] B. J. Zhang and S. J. Jeon, Chem. Phys. Lett. **377**, 210 (2003).
[22] C. L. Thomsen, D. Madsen, S. R. Keiding, J. Thøgersen, and O. Christiansen, J. Chem. Phys. **110**, 3453 (1999).
[23] D. N. Nikogosyan, A. A. Oraevsky, and V. I. Rapusov, Chem. Phys. **77**, 131 (1983).
[24] A. Reuther, A. Laubereau, and D. N. Nikogosyan, J. Chem. Phys. **100**, 16794 (1996).
[25] S. Pommeret, F. Gobert, M. Mostafavi, I. Lampre, and J.-C. Mialocq, J. Phys. Chem. A **105**, 11400 (2001).
[26] A. Dragomir, J. G. McInerney, D. N. Nikogosyan, and L. A. Ruth, IEEE J. Quantum Electron. **38**, 31 (2002).
[27] M. J. Paterson, O. Christiansen, F. Pawłowski, P. Jørgensen, C. Hättig, T. Helgaker, and P. Sałek, J. Chem. Phys. **124**, 054322 (2006).
[28] C. B. Nielsen, S. Rettrup, and S. P. A. Sauer, J. Chem. Phys. **124**, 114108 (2006).
[29] T. D. Poulsen, P. R. Ogilby, and K. V. Mikkelsen, J. Phys. Chem. A **103**, 3418 (1999).
[30] T. Keszthelyi, T. D. Poulsen, P. R. Ogilby, and K. V. Mikkelsen, J. Phys. Chem. A **104**, 10550 (2000).
[31] C. S. Foote, Acc. Chem. Res. **1**, 104 (1968).
[32] *Singlet Oxygen*, edited by A. A. Frimer (CRC, Boca Raton, FL, 1985), Vols. I–IV.
[33] P. K. Frederiksen, M. Jørgensen, and P. R. Ogilby, J. Am. Chem. Soc. **123**, 1215 (2001).
[34] S. P. McIlroy, E. Cló, L. Nikolajsen, P. K. Frederiksen, C. B. Nielsen, K. V. Mikkelsen, K. V. Gothelf, and P. R. Ogilby, J. Org. Chem. **70**, 1134 (2005).
[35] P. K. Frederiksen, S. P. McIlroy, C. B. Nielsen, L. Nikolajsen, E. Skovsen, M. Jørgensen, K. V. Mikkelsen, and P. R. Ogilby, J. Am. Chem. Soc. **127**, 255 (2005).
[36] C. B. Nielsen, M. Johnsen, J. Arnbjerg, M. Pittelkow, S. P. McIlroy, P. R. Ogiby, and M. Jørgensen, J. Org. Chem. **70**, 7065 (2005).
[37] O. Christiansen, P. Jørgensen, and C. Hättig, Int. J. Quantum Chem. **68**, 1 (1998).
[38] O. Christiansen, H. Koch, and P. Jørgensen, Chem. Phys. Lett. **243**, 409 (1995).
[39] G. D. Purvis and R. J. Bartlett, J. Chem. Phys. **76**, 1910 (1982).
[40] P. Linse, MOLSIM, Version 3.3.0, University of Lund, Sweden, 2001.
[41] G. D. Billing and K. V. Mikkelsen, Chem. Phys. **182**, 249 (1994).
[42] J. Kongsted, A. Osted, T. B. Pedersen, K. V. Mikkelsen, and O. Christiansen, J. Phys. Chem. A **108**, 8624 (2004).
[43] P. Ahlström, A. Wallqvist, S. Engström, and B. Jönnson, Mol. Phys. **68**, 563 (1989).
[44] J. T. Blair, K. Krogh-Jespersen, and R. M. Levy, J. Am. Chem. Soc. **111**, 6948 (1989).
[45] S. J. Wiener, P. A. Kollman, D. A. Case, U. C. Singh, C. Ghio, G. Alagona, S. Profeta, Jr., and P. Weiner, J. Am. Chem. Soc. **106**, 765 (1984).
[46] J. Kongsted, A. Osted, K. V. Mikkelsen, and O. Christiansen, J. Chem. Phys. **118**, 1620 (2002).
[47] J. Kongsted, A. Osted, K. V. Mikkelsen, and O. Christiansen, J. Chem. Phys. **119**, 10519 (2003).
[48] J. Kongsted, A. Osted, K. V. Mikkelsen, and O. Christiansen, J. Chem. Phys. **120**, 3787 (2004).
[49] A. Osted, J. Kongsted, K. V. Mikkelsen, P.-O. Åstrand, and O. Christiansen, J. Chem. Phys. **124**, 124503 (2006).
[50] J. Kongsted, A. Osted, K. V. Mikkelsen, and O. Christiansen, Mol. Phys. **100**, 1813 (2002).
[51] J. Kongsted, A. Osted, K. V. Mikkelsen, and O. Christiansen, J. Phys. Chem. A **107**, 2578 (2003).
[52] B. T. Thole and P. Th. van Duijnen, Chem. Phys. **71**, 211 (1982).
[53] W. J. Meath and E. A. Power, J. Phys. B **7**, 763 (1984).
[54] C. Hättig, O. Christiansen, and P. Jørgensen, J. Chem. Phys. **108**, 8355 (1998).
[55] C. Hättig, O. Christiansen, and P. Jørgensen, J. Chem. Phys. **108**, 8331 (1998).
[56] P. R. Monson and W. M. McClain, J. Chem. Phys. **53**, 29 (1970).
[57] DALTON, a molecular electronic structure program, Release 2.0, 2005, http://www.kjemi.uio.no/software/dalton/dalton.html
[58] O. Christiansen, MIDASCPP, molecular interactions, dynamics, and simulation in C++, 2004.
[59] A. Ligabaue, S. P. A. Sauer, and P. Lazzeretti, J. Chem. Phys. **118**, 6830 (2003).
[60] J. Kongsted, A. Osted, K. V. Mikkelsen, P.-O. Åstrand, and O. Christiansen, J. Chem. Phys. **121**, 8435 (2004).
[61] K. Aidas, J. Kongsted, A. Osted, K. V. Mikkelsen, and O. Christiansen, J. Phys. Chem. A **109**, 8001 (2005).
[62] S. Hirata, M. Valiev, M. Dupuis, S. S. Xantheas, S. Sugiki, and H. Sekino, Mol. Phys. **103**, 10 (2005).
[63] M. D'Abramo, M. Aschi, A. Di Nola, and A. Amadei, Chem. Phys. Lett. **424**, 289 (2006).
[64] M. L. Sánchez, M. E. Martín, M. A. Aguilar, and F. J. Olivares del Valle, Chem. Phys. Lett. **310**, 195 (1999).
[65] A. Osted, J. Kongsted, K. V. Mikkelsen, and O. Christiansen, J. Phys. Chem. A **108**, 8646 (2004).
[66] J. Kongsted, A. Osted, K. V. Mikkelsen, and O. Christiansen, in *Atoms, Molecules And Clusters in Electric Fields: Theoretical Approaches to the Calculation of Electric Polarizability*, edited by G. Maroulis (Imperial College Press, London, 2005).
[67] O. Christiansen, T. M. Nymand, and K. V. Mikkelsen, J. Chem. Phys. **113**, 8101 (2000).
[68] R. Schinke, *Photodissociation Dynamics* (Cambridge University Press, Cambridge, 1993).

Downloaded 08 Nov 2006 to 137.195.101.208. Redistribution subject to AIP license or copyright, see http://jcp.aip.org/jcp/copyright.jsp

[69] J. M. Heller, R. N. Hamn, R. D. Birkhoff, and L. R. Painter, J. Chem. Phys. **60**, 3483 (1974).
[70] H.-t. Wang, W. S. Felps, and S. P. McGlynn, J. Chem. Phys. **67**, 2614 (1977).
[71] R. B. Robin, *Higher Excited States of Polyatomic Molecules*, 3rd ed. (Academic, New York, 1985), Vol. III.
[72] R. E. Verrall and W. A. Senior, J. Chem. Phys. **50**, 2746 (1969).
[73] M. Aschi, M. D'Abramo, C. Di Teodoro, A. Di Nola, and A. Amadei, ChemPhysChem **6**, 53 (2005).
[74] B. D. Bursulaya, J. Jeon, C.-N. Yang, and H. J. Kim, J. Phys. Chem. A **104**, 45 (2000).
[75] W. F. Chan, G. Cooper, and C. E. Brion, Chem. Phys. **178**, 387 (1993).

Downloaded 08 Nov 2006 to 137.195.101.208. Redistribution subject to AIP license or copyright, see http://jcp.aip.org/jcp/copyright.jsp